Cerebral Cortex, February 2017;27: 1326–1336

doi:10.1093/cercor/bhv322
Advance Access Publication Date: 4 January 2016
Original Article

ORIGINAL ARTICLE

Genetic Variation in S100B Modulates Neural Processing of Visual Scenes in Han Chinese

Xiang-zhen Kong[1,3,†], Yiying Song[1,3,†], Zonglei Zhen[1,3] and Jia Liu[2,3]

[1]State Key Laboratory of Cognitive Neuroscience and Learning & IDG/McGovern Institute for Brain Research, [2]School of Psychology and [3]Center for Collaboration and Innovation in Brain and Learning Sciences, Beijing Normal University, Beijing 100875, China

Address correspondence to Jia Liu, Room 405, Yingdong Building, 19 Xinjiekouwai St, Haidian District, Beijing 100875, China. Email: liujia@bnu.edu.cn

[†]X.Z.K. and Y.S. contributed equally to this study.

Abstract

Spatial navigation is a crucial ability for living. Previous animal studies have shown that the S100B gene is causally related to spatial navigation performance in mice. However, the genetic factors influencing human navigation and its neural substrates remain unclear. Here, we provided the first evidence that the S100B gene modulates neural processing of navigationally relevant scenes in humans. First, with a novel protocol, we demonstrated that the spatial pattern of S100B gene expression in postmortem brains was associated with brain activation pattern for spatial navigation in general, and for scene processing in particular. Further, in a large fMRI cohort of healthy adults of Han Chinese ($N = 202$), we found that S100B gene polymorphisms modulated scene selectivity in the retrosplenial cortex (RSC) and parahippocampal place area. Finally, the serum levels of S100B protein mediated the association between S100B gene polymorphism and scene selectivity in the RSC. Our study takes the first step toward understanding the neurogenetic mechanism of human spatial navigation and suggests a novel approach to discover candidate genes modulating cognitive functions.

Key words: cortical scene processing, genetics, S100B, single nucleotide polymorphism, spatial navigation

Introduction

Spatial navigation is a crucial ability for creatures. Good navigation ability increased the survival rate for our ancestors, and even in modern life, better navigation ability improves our journey during travel. Previous animal studies have shown that the S100B gene is causally related to spatial navigation in mice. For instance, mutant mice with null S100B gene expression exhibit enhanced navigation performance in the water maze test (Nishiyama et al. 2002), while transgenic mice with over-expression of S100B gene show impaired behavior in navigation (Gerlai et al. 1995). However, whether S100B gene influences neural processing of spatial navigation in the human brain, and the mechanism by which it does so, remains unclear.

Perception of surrounding scenes is a critical component of successful navigation in a complex environment. Neuroimaging studies have identified several cortical regions selective for scene processing in the human brain, including the parahippocampal place area (PPA) in the posterior parahippocampal cortex (Epstein et al. 1999), the retrosplenial cortex (RSC) in the parietaloccipital sulcus (Maguire 2001), and the occipital place area (OPA, also known as "TOS") in transverse occipital sulcus (Grill-Spector 2003; Dilks et al. 2013). These regions respond more strongly during viewing of navigationally relevant scenes compared with viewing of non-scene stimuli (e.g., objects) (Aguirre et al. 1998; Epstein and Kanwisher 1998; Nakamura et al. 2000; Hasson et al. 2003). Previous studies indicated that these regions play a pivotal role in human spatial navigation (Epstein 2008). For example, functional magnetic resonance imaging (fMRI) studies have shown that these regions are activated in mental and virtual navigation tasks (Ghaem et al. 1997; Maguire et al. 1998; Ino et al.

2002; Rosenbaum et al. 2004; Spiers and Maguire 2006; Rauchs et al. 2008). Moreover, lesions in these regions (e.g., PPA and RSC) often lead to deficits in way-finding (Aguirre and D'Esposito 1999; Epstein et al. 2001; Mendez and Cherrier 2003). Together with the association between the S100B gene and spatial navigation revealed in animal studies, we hypothesized that the S100B gene may modulate cortical scene processing in the human brain, especially in these scene-selective regions.

To test our hypothesis, we used a novel approach (see also Gorgolewski et al. [2014]) to explore the association between the S100B gene and neural processing of navigation. Specifically, we examined the spatial similarity between the S100B gene expression map (from the Allen Human Brain Atlas, AHBA) (Hawrylycz et al. 2012) and an activation map of navigation based on a large-scale neuroimaging meta-analysis (from the Neurosynth) (Yarkoni et al. 2011). After obtaining the association, we investigated whether scene processing, the first and critical component of spatial navigation, was modulated by the S100B gene; this was done by examining whether the spatial pattern of S100B gene expression was related to that of brain activation during viewing of natural scenes derived from a large cohort of participants (N = 202). Further, we examined whether single nucleotide polymorphisms (SNPs) in the S100B gene modulated scene selectivity in the scene-selective regions. Finally, we examined whether the serum level of the S100B protein, a proxy of S100B gene expression level in the brain (Reiber 2001; Rothermundt et al. 2004), mediated the observed gene-brain association.

Materials and Methods

Participants

Two hundred and two college students (124 females; mean age = 20.3 years, standard deviation [SD] = 0.83 years) from Beijing Normal University (BNU), Beijing, China, participated in the study. The sample size was determined based on 2 prior studies (Hohoff et al. 2010; Dagdan et al. 2011), where reliable associations between S100B gene and serum S100B levels were revealed in healthy adults with the sample size of ~200. The participants were recruited through advertisement on campus, and all of them are Han Chinese. All participants had no history of neurological or psychiatric disorders and had normal or corrected-to-normal vision. The dataset is part of the Brain Activity Atlas Project (BAA, http://www.brainactivityatlas.org/). The study was approved by the Institutional Review Board of BNU. Written informed consent was obtained from all participants before they took part in the experiment.

All participants (N = 202) underwent the fMRI scanning, and no participant was excluded due to excessive head motion (2 mm in translation or 2° in rotation from the first volume in any axis) or visually detected registration errors (Zhen et al. 2015). In addition, most of these participants (N = 187; 111 females; mean age = 20.3 years, SD = 0.90 years) volunteered to provide venous blood samples for S100B SNP genotyping and serum S100B measurement. Ten participants with undetermined genotypes for any SNP were excluded during SNP genotyping, leaving 177 participants (103 females; mean age = 20.3 years, SD = 0.93 years) to be included for SNP analyses. No participant was excluded during serum S100B measurement, leaving all 187 participants to be included for serum analyses.

Stimuli and fMRI Scanning

The stimuli used in the fMRI scanning contained colored movie clips of 4 object categories (i.e., scenes, faces, objects and scrambled objects) (Pitcher et al. 2011; Dilks et al. 2013). Movie clips of scenes were mostly pastoral scenes shot from a car window while driving slowly through leafy suburbs, along with some other films taken while flying through canyons or walking through tunnels. Movie clips of faces were filmed on a black background and framed close-up to reveal only the faces of 7 children as they danced or played with toys or adults (who were out of frame). Movie clips of objects showed moving toys, which were included to examine cortical selectivity to scenes and faces. The movie clips of scrambled objects were constructed by scrambling each frame of the object movie clips (for more details on the stimuli, see Pitcher et al. [2011]).

Each participant took part in a session of 3 blocked-design fMRI runs. Each run lasted 3 min 18 s, and consisted of 2 block sets intermixed with 3 18-s rest blocks at the beginning, middle, and end of the run. Each block set consisted of 4 blocks, with 1 stimulus category presented in each 18-s block. Each block contained 6 3-s movie clips from a stimulus category, which were randomly drawn from a pool of 60 clips. The order of stimulus category blocks in each run was palindromic and was randomized across runs. During scanning, subjects were instructed to passively view the movie clips.

fMRI Data Acquisition

Scanning was conducted at BNU Imaging Center for Brain Research, Beijing, China, on a Siemens 3T scanner (MAGENTOM Trio, a Tim system) with a 12-channel phased-array head coil. Functional blood-oxygen-level-dependent images were acquired with a T2*-weighted gradient-echo, echo-planar-imaging (GRE-EPI) sequence (TR/TE = 2000/30 ms; flip angle = 90°, in-plane resolution = 3.1 × 3.1 mm). Whole-brain coverage for the functional data was obtained using 30 contiguous interleaved 4.8 mm axial slices. Structural T1-weighted images were acquired with a 3D magnetization-prepared rapid acquisition gradient-echo (MP-RAGE) scan (TR/TE/TI = 2530/3.39/1100 ms, flip angle = 7°) for spatial normalization and anatomically localizing the functional activations.

fMRI Data Analysis

Data were analyzed using imaging tools available in the Functional MRI of the Brain's Software Library (FSL, http://www.fmrib.ox.ac.uk/fsl) and in-house Python-coded utilities. For the functional data, the first-level analysis was conducted separately for each run and each session. Preprocessing included the following steps: high-pass temporal filtering (120-s cutoff), motion correction, brain extraction, spatial smoothing (Gaussian kernel, FWHM = 6 mm), and grand-mean intensity normalization. Statistical analyses on time series were performed using FILM (FMRIB's Improved Linear Model) with a local autocorrelation correction. The general linear model modeled the scene, face, object, and scrambled object stimuli as explanatory variables (EVs), convolved with a hemodynamic response function. Within the time course of each EV, the onset and duration of every stimulus was modeled. The temporal derivative of each EV was modeled to improve the sensitivity of the model. Six parameters from motion-correction were also included in the model as confounding variables to account for the effect of residual head movements. Statistical contrasts between pairs of different stimulus categories were evaluated.

After the first-level analysis, all runs within each session were combined during the second-level analysis. Specifically, the parameter (i.e., beta) images from the first-level analysis were firstly aligned to the structural images of one's own through FLIRT

(FMRIB's linear image registration tool) with 6° of freedom and then warped to the MNI152 template through FNIRT (FMRIB's nonlinear image registration tool) with the default parameters. The spatially normalized parameter images (resampled to 2-mm isotropic voxels) were then summarized across runs in each session using a fixed-effects model. The statistic images from the second-level analysis were then used to create the probabilistic activation map and extract individual's scene selectivity (see below).

Probabilistic Activation Map

The Probabilistic Activation Map (PAM) for scene processing was created by overlaying the z-statistic maps from all participants for the contrast of scenes versus objects onto the MNI152 template, and then dividing by the total number of participants (e.g., Zhen et al. 2013). The value for each voxel in the map indicated the probability of the voxel showing a significantly higher response for scenes than for objects ($Z > 2.3$, $P < 0.01$ uncorrected) across population. As a control, the PAM for face processing was created under the contrast of faces versus objects with the same procedure.

Delineation of Scene-Selective Regions

Further, we identified 3 well-established scene-selective regions as the regions of interest (ROIs) by thresholding the PAM, including the PPA, RSC, and OPA. The PAM for scene processing was thresholded at 30% (i.e., >30% participants showed scene selectivity) and segmented into several clusters using watershed segmentation codes developed in Python (available in the scikits-image project, http://scikits-image.org). The PPA for each hemisphere was defined as a set of contiguous voxels localized in the posterior parahippocampus gyrus (Epstein et al. 1999). The RSC and OPA were defined in the same way but localized in the parietaloccipital sulcus (Maguire 2001) and the transverse occipital sulcus (Grill-Spector 2003; Dilks et al. 2013), respectively. Locations and sizes of these scene-selective regions are shown in Table 1.

S100B Gene SNPs Genotyping

The human S100B gene is located on chromosome 21q22.3. Five S100B gene SNPs were taken as candidate SNPs. First, previous studies have shown that rs3788266 (at 5′-UTR) modulates the S100B gene expression and is associated with serum levels of S100B protein (Roche et al. 2007; Dagdan et al. 2011). Second, Hohoff et al. (2010) identified the association of rs11542311 (at exon 2) with S100B serum levels and S100B mRNA expression (Hohoff et al. 2010). In addition, to cover the full length of S100B gene, tag SNPs were selected from the Han Chinese in Beijing in the HapMap database (http://www.hapmap.org/, HapMap Data Rel 27 Phase II + III) using the Tagger program (S100B gene and its 2 kb upstream and downstream region as the region of interest; SNPs with minor allele frequency [MAF] <20% excluded, and pair-wise tagging with r^2 threshold of 0.80) (de Bakker et al. 2005). Thus, 3 other SNPs (rs2839349 at 3′-UTR, rs2839357 at intron 1, and rs881827 at intron 2) were included into the genotyping analyses.

Genomic DNA was extracted from 200ul venous blood sample of each subject using the QuickGene-Mini80 equipment and QuickGene DNA whole blood kit S (Fujifilm). All the SNPs were genotyped using Taqman allele-specific assays on the 7900HT Fast Real-Time PCR System (Applied Biosystems). Genotypes were determined automatically. The Hardy–Weinberg test was performed for each SNP using the PLINK program (Purcell et al. 2007). In addition, the allele frequencies in our sample were very similar to those of the Han Chinese sample in the HapMap dataset (HapMap Data Release 27 Phase II + III). All SNPs met the following criteria: MAF >0.10, Hardy–Weinberg equilibrium (HWE) $P > 0.05$, and genotyping call rate >0.95.

Table 1 MNI coordinates and size of the scene-selective regions

Brain region	Hemi	Peak MNI coordinates	Cluster size (voxel)
PPA	L	−26, −46, −8	865
	R	24, −42, −10	910
RSC	L	−10, −54, 4	1506
	R	14, −50, 4	1371
OPA	L	−40, −80, 34	443
	R	50, −68, 34	330

L, left; R, right.

The Serum Levels of S100B Protein

Peripheral venous samples were collected in serum separator tubes following an overnight fast. The plasma samples were separated within 2 h by centrifugation, and serum was isolated and stored at −70°C until the samples were analyzed. Serum levels of S100B protein were measured using a commercially available ELISA kit as described previously (Qi et al. 2009). Mean serum S100B level in our sample (0.15 ± 0.037 μg/L) was in the normal range of healthy subjects (Portela et al. 2002) and showed no sex difference, $t_{(185)} < 1.0$.

Navigation Map from the Meta-Analysis with the Neurosynth

To obtain the activation map relevant for spatial navigation, we used an automated meta-analysis tool, Neurosynth (https://github.com/neurosynth/neurosynth) (Yarkoni et al. 2011), to generate the reverse inference map which shows the likelihood that the term "navigation" was used in a study if activation was reported at a particular voxel. Neurosynth uses text-mining techniques to detect frequently used terms (as proxies for concepts of interest) in the neuroimaging literature: terms that occur at a high frequency in a given study are then associated with all activation coordinates in this publication, allowing for automated term-based meta-analysis. Despite the automaticity and the potentially high noise resulting from the association between term frequency and coordinate tables, this approach has been shown to be quite robust and reliable (e.g., Yarkoni et al. 2011; Helfinstein et al. 2014). The database was accessed on 7 November 2014, searching for the feature "navigation" (55 studies with 2765 activations; 91% of these studies were conducted in North America and Europe according to the authors' affiliations). As expected, the resulting statistical map included the hippocampus, parahippocampal gyrus, and RSC, which have been revealed in previous navigation studies (e.g., Ohnishi et al. 2006; Sherrill et al. 2013).

S100B Gene Expression in Postmortem Human Brain

In this study, S100B gene expression across the brain was extracted from the Allen Human Brain Atlas (http://www.brain-map.org), a publicly available online resource for gene expression. The atlas characterizes gene expression in postmortem human brain with genome-wide microarray-based gene expression

profiles including over 62 000 gene probes for 500 sampling sites from each hemisphere covering the whole brain (See Hawrylycz et al. [2012] for more details about the data collection). Microarray analysis data, normalized across each individual brain, are included in the gene expression dataset. The normalized scores represent regional gene expression of that sampling site normalized to whole-brain expression of a specific gene. To date (search conducted on the 9 July 2014), 6 adult donors with no history of neuropsychiatric or neurological conditions are available in the database (age 24, 31, 34, 49, 55, and 57 years; 1 female). Among these 6 donors, 3 are Caucasian, 2 are African American, and 1 is Hispanic. Detailed information for donors included and analysis methods is available at www.brain-map.org. Furthermore, structural brain imaging data of each donor were used to visualize gene expression data in its native three-dimensional anatomical coordinate space, allowing for correlation analysis between the spatial distributions of fMRI data and gene expression.

The Combined fMRI and Gene Expression Analysis

First, we extracted the values of the normalized S100B gene expression for each sampling site and each donor using the Allen Brain Institute REST API (http://www.brain-map.org/). Note that gene expression of S100B was analyzed with 2 probes (i.e., A_23_P143526 and CUST_17042_PI416261804) in the Allen Human Brain Atlas, and values of the 2 probes were averaged to estimate S100B expression. This provides a vector of the normalized gene expression values in a set of sampling sites, representing the spatial distribution of S100B gene expression across the brain of each donor (Fig. 1A for a typical donor, donor ID: H0351.2002).

We next translated the location of each sampling site to MNI space with nonlinear co-registration and drew a spherical ROI centered on the sampling site ($r = 4$ mm) using the alleninfo tool (https://github.com/chrisfilo/alleninf) (Gorgolewski et al. 2014). For each spherical ROI, we extracted and averaged the statistical values of all voxels within the ROI from the navigation map based on the meta-analysis. This provides a vector of the statistical values of the ROIs centered on the sampling sites, representing the spatial distribution of the activation likelihood relevant to navigation across the brain.

To examine the spatial similarity of the S100B gene expression map and the navigation map, the approximate random effect analysis from the *alleninfo* (Gorgolewski et al. 2014) was performed. Briefly, we first correlated the spatial distribution of S100B gene expression of each donor with that of the navigation map, getting a slope of best linear fit for each donor, and then performed a one-sample t-test on those estimates. The random effects model allows us to test whether the results can be generalized beyond the 6 donors to the whole population.

The same method was used to investigate the association between S100B gene expression and cortical scene processing, except this test used the PAM for scene processing from our participants instead of the navigation map from meta-analysis. For each spherical ROI, we extracted and averaged the activation probability values for all voxels within the ROI from the PAM for scene processing. The approximate random effect analysis was constrained within the regions showing reliable activation during scene processing across participants (PAM >30%). As a control, we also conducted the same analysis with the face PAM.

The Combined fMRI and SNP Analysis

To explore the association between the S100B gene SNPs and regional scene selectivity, we compared the scene selectivity between participants with different genotypes for each candidate SNP for each voxel in the predefined scene-selective ROIs. There were 3 pair-wise comparisons for each SNP (e.g., for the SNP rs11542311: CC versus GG, CC versus CG, and GG versus CG), and therefore, 15 comparisons for all 5 SNPs in each voxel. We controlled for age and gender in these analyses. To perform the multiple comparisons correction, the voxel-wise intensity threshold was set at $P < 0.005$ and the alpha threshold was set at *alpha* <0.0033 (0.05/15). Next, the cluster-level threshold within each ROI was calculated using 3dClustSim from AFNI (http://afni.nimh.nih.gov/afni/), with Monte Carlo simulation (Ward 2000).

Additionally, simplified SNP models were fitted for each SNP that showed a significant association with scene selectivity: a dominant model (the major allele homozygous was given a score of 1, and the heterozygous grouped with the minor allele homozygous was given a score of −1, e.g., for rs11542311: GG = 1, CC/CG = −1), a recessive model (the minor allele homozygous was given score of 1, and the heterozygous grouped with the major allele homozygous was given a score of −1, e.g., for rs11542311: CC = 1, CG/GG = −1), and an additive model (a score was assigned by counting the number of minor alleles: the homozygote for the major allele was given a score of 0, the heterozygote was given a score of 1, and the homozygote for the minor allele was given a score of 2;, e.g., for rs11542311: GG = 0, CG = 1, CC = 2). For each candidate model, the analysis was conducted with a linear regression model, in which genotype was entered as independent variable, regional scene selectivity was entered as dependent variable, and gender and age were entered as covariates. All the analyses were done using SPSS version 18.0. False discovery rate correction for multiple comparisons was used.

Finally, we explored the potential pathway of the observed gene-neural association through the S100B protein. First, we calculated the partial correlation between the serum levels of S100B protein and scene selectivity in the clusters modulated by the S100B genotype, with sex and age controlled. Second, we examined the association between S100B SNP genotypes and the serum levels of S100B protein. Finally, a mediation analysis was performed with SNP genotypes, serum levels of S100B protein, and regional scene selectivity as the predictor, mediator, and outcome, respectively (Wager et al. 2008). Age and gender were treated as covariates in the model. A bootstrapping procedure was applied to obtain an unbiased estimate of the indirect effect and a 95% confidence interval (CI). If the 95% CI did not contain zero, the indirect effect was considered significant (i.e., $P < 0.05$). In addition, we calculated the proportion of variances mediated by serum S100B level in the mediation model (MacKinnon et al. 2007).

Results

S100B Gene Expression was Associated with Brain Activation of Navigation in Humans

We first explored the possible involvement of the S100B gene in human spatial navigation by examining the similarity between the S100B gene expression map and the activation map for navigation. The S100B gene expression map was obtained from the AHBA (Fig. 1A), and the navigation map was obtained from a neuroimaging meta-analysis with Neurosynth (Fig. 1B). We found a consistent negative association between the spatial pattern of the S100B gene expression map and that of the navigation map across all 6 donors of the AHBA (Fig. 1E, for a typical donor; beta = −0.19; $r = -0.25$, $P < 0.001$). Moreover, the random effects model confirmed that the results could be generalized beyond the 6

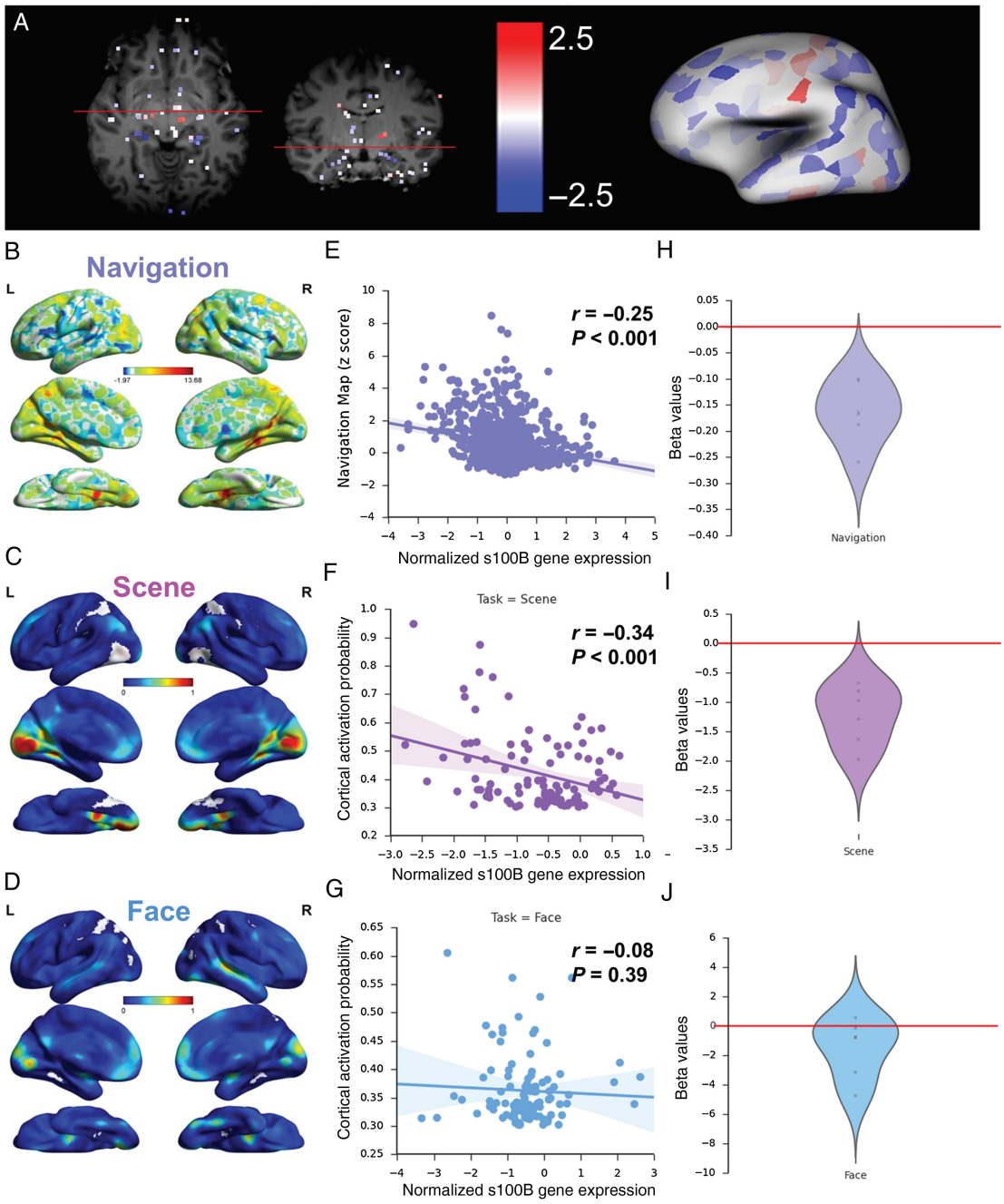

Figure 1. Association between the S100B gene expression map and brain activation map for human navigation. (*A*) Left: The sampling site and normalized S100B gene expression in a typical donor from the AHBA; Right: The gene expression data are rendered on the surface of a brain template. (*B*) The navigation map from a meta-analysis with Neurosynth. (*C*) The activation probability map for scene processing and (*D*) for face processing from our participants. (*E*) Spatial correlation between the S100B gene expression map in a typical donor and the navigation map, (*F*) scene activation probability map, and (*G*) face activation probability map. (*H*) Beta value distribution of the linear regression between the S100B gene expression map and the navigation map, (*I*) scene activation probability map, and (*J*) face activation probability map for all 6 donors.

donors to the whole population (Fig 1*H*; $t = -6.77$, $P = 0.001$). That is, regions with lower S100B gene expression were more likely to be activated in navigation-related tasks. Notably, the negative correlation between S100B gene expression and navigation activation fits nicely with animal studies showing a negative association between S100B gene expression and navigation performance (Gerlai et al. 1995; Nishiyama et al. 2002). Because spatial navigation is a complex cognitive function consisting of multiple components, such as scene recognition, localization and orientation, accessing long-term spatial representations, and route planning (Shah and Miyake 2005; Wolbers and Hegarty 2010; Epstein and Vass 2014), we next focused on scene processing, the first and critical component of spatial navigation.

To do this, we correlated the S100B gene expression map with the activation probability map derived from fMRI data when participants viewed natural scenes (Fig. 1*C*). Similar to the

aforementioned association, we found a negative correlation between the S100B gene expression map of each donor and the scene-selective activation probability map reliably activated during scene processing derived from our participants (Fig. 1F left for a typical donor, beta = –1.97; $r = -0.34$, $P < 0.001$). The random effects model showed that the association could be generalized beyond the 6 donors (Fig. 1I right; $t = -5.99$, $P = 0.002$). That is, regions with lower S100B gene expression were more likely to be activated during scene processing.

To examine the specificity of the association between S100B gene expression and scene processing, we asked whether the S100B gene expression map was also associated with the activation probability map when participants viewed faces (Fig. 1D). We found that the association was discrepant across the donors (Fig. 1G left for a typical donor, beta = –0.45; $r = -0.08$, $P = 0.39$), and random effects analysis showed that the association was not significant at group level (Fig. 1J right; $t < 1.00$). Taken together, these results indicate that the S100B gene may be selectively involved in modulating cortical processing of scenes.

S100B Gene Polymorphisms Modulated Cortical Scene Selectivity

Next, we asked what specific S100B gene polymorphisms modulate cortical processing of scenes. Based on the functions and locations of the S100B gene SNPs reported in previous studies (Roche et al. 2007; Hohoff et al. 2010; Dagdan et al. 2011; Zhai et al. 2012), 5 candidate SNPs, including rs3788266, rs11542311, rs2839349, rs881827, and rs2839357, were selected. Genotype frequency for each candidate SNP and demographic information of each genotype groups are shown in Table 2. No deviation from the HWE was found in the sample (P values > 0.30), and all genotype groups were matched for age and gender (P values > 0.15). To relate the S100B gene polymorphisms to cortical scene selectivity, we conducted voxel-wise analysis within 3 well-established scene-selective regions, the PPA, RSC, and OPA, to compare scene selectivity between participants with different genotypes for the 5 candidate SNPs.

Table 2 Distribution of the S100B genotype groups and demographic information

SNP ID	N	Sex	Age (years)
rs2839349			
AA	77 (43.5%)	41F/36M	20.17 ± 0.96
AG	77 (43.5%)	45F/32M	20.25 ± 0.83
GG	23 (13.0%)	17F/6M	20.60 ± 1.07
rs881827			
AA	22 (12.4%)	11F/11M	20.23 ± 1.12
AG	76 (42.9%)	45F/31M	20.18 ± 0.83
GG	79 (44.6%)	47F/32M	20.35 ± 0.96
rs11542311			
CC	30 (16.9%)	18F/12M	20.25 ± 0.92
CG	94 (53.1%)	57F/37M	20.28 ± 0.95
GG	53 (29.9%)	28F/25M	20.24 ± 0.92
rs2839357			
AA	89 (50.3%)	54F/35M	20.30 ± 0.92
AG	72 (40.7%)	41F/31M	20.23 ± 0.95
GG	16 (9.0%)	8F/8M	20.19 ± 0.93
rs3788266			
AA	9 (5.1%)	6F/3M	20.40 ± 0.99
AG	70 (39.5%)	40F/30M	20.33 ± 0.97
GG	98 (55.4%)	57F/41M	20.21 ± 0.90

F, female; M, male.

After controlling for age and gender, 4 clusters in 2 scene-selective regions showed significant differences in scene selectivity between participants with different genotypes (corrected $P \leq 0.0033$ [0.05/15]). Specifically, a cluster in the posterior part of the right RSC (prRSC) showed different scene selectivity between 2 genotypes of rs11542311 (CC > CG: MNI coordinates [18, –54, –2], Z-value = 3.04, $P = 0.0012$, 288 mm^3; Fig. 2A Red). Two comparisons of rs3788266 genotypes (AA > AG; AA > GG) showed different scene selectivity in 2 clusters in the anterior part of the right RSC (MNI coordinates [16, –48, 4], Z-value = 3.25, $P = 0.00058$, 264 mm^3; MNI coordinates [22, –50, 12], Z-value = 2.99, $P = 0.0014$, 264 mm^3, respectively). Because these 2 clusters were largely overlapped (~80%), we used their intersection as the anterior ROI (arRSC: Center MNI coordinates [12, –46, 5], 208 mm^3; Fig. 2A Blue) in the following analyses. Finally, a cluster in the left PPA (lPPA) showed different scene selectivity between genotypes of rs3788266 (AA > AG: MNI coordinates [–16, –40, –10], Z-value = 3.57, $P = 0.00018$, 1056 mm^3; Fig. 2A Green). No significant association was found in other regions.

To further illustrate how the S100B gene polymorphisms modulate cortical scene selectivity, 3 SNP models were examined: a dominant model, a recessive model, and an additive model. Overall, we found that only the recessive model fitted the association between the S100B SNPs and scene selectivity in the identified clusters (rs11542311 and prRSC: $t = 2.80$, $P = 0.006$, Fig. 2B Left; rs3788266 and arRSC: $t = 3.36$, $P = 0.001$, Fig. 2B Middle; rs3788266 and lPPA: $t = 3.52$, $P = 0.001$; Fig. 2B Right). In other words, homogenous A-allele carriers of rs3788266 showed significantly higher scene selectivity than G-allele carries in both the arRSC and the lPPA (AA > AG + GG), and homogenous C-allele carriers of rs11542311 showed significantly higher scene selectivity than G-allele carries in the prRSC (CC > CG + GG). Other SNP models did not generate any significant results (rs11542311 and prRSC, dominant model: $t = -0.035$, $P = 0.725$; additive model: $t = 1.30$, $P = 0.197$; rs3788266 and arRSC, dominant model: $t = 0.61$, $P = 0.545$; additive model: $t = 1.73$, $P = 0.085$; rs3788266 and lPPA, dominant model: $t = 0.39$, $P = 0.697$; additive model: $t = 0.94$, $P = 0.351$).

Serum S100B Levels Mediated the Relation Between S100B Gene and Scene Selectivity

Finally, we explored whether the S100B SNPs, rs11542311, and rs3788266 modulated scene selectivity in the arRSC, prRSC, and lPPA through its gene product, the S100B protein. Previous studies have demonstrated that rs11542311 and rs3788266 directly modulate the serum levels of S100B protein (Hohoff et al. 2010; Dagdan et al. 2011); here, we asked whether the serum levels of S100B protein mediated the association between the S100B SNPs and cortical scene selectivity. First, as reported in previous studies (Roche et al. 2007; Dagdan et al. 2011), significantly lower serum levels of S100B protein were found in homogenous A-allele carriers than in G-allele carries of rs3788266 (AA versus AG + GG: $t = -2.67$, $P = 0.022$, Bonferroni-corrected $P < 0.05$; Fig 3B). In contrast, variation in rs11542311 was not related to the serum levels of S100B protein (CC versus CG + GG: $t = 1.26$, $P = 0.216$, uncorrected). Further, we found that the serum levels of S100B protein were negatively correlated with scene selectivity in the arRSC ($r = -0.18$, $P = 0.021$; Fig. 3A), but not in the prRSC ($r = -0.13$, $P = 0.090$) or lPPA ($r = -0.12$, $P = 0.134$). Therefore, we focused on rs3788266 and the arRSC in the mediation analysis.

The mediation analysis showed that the differences in scene selectivity in the arRSC between homogenous A-allele carriers

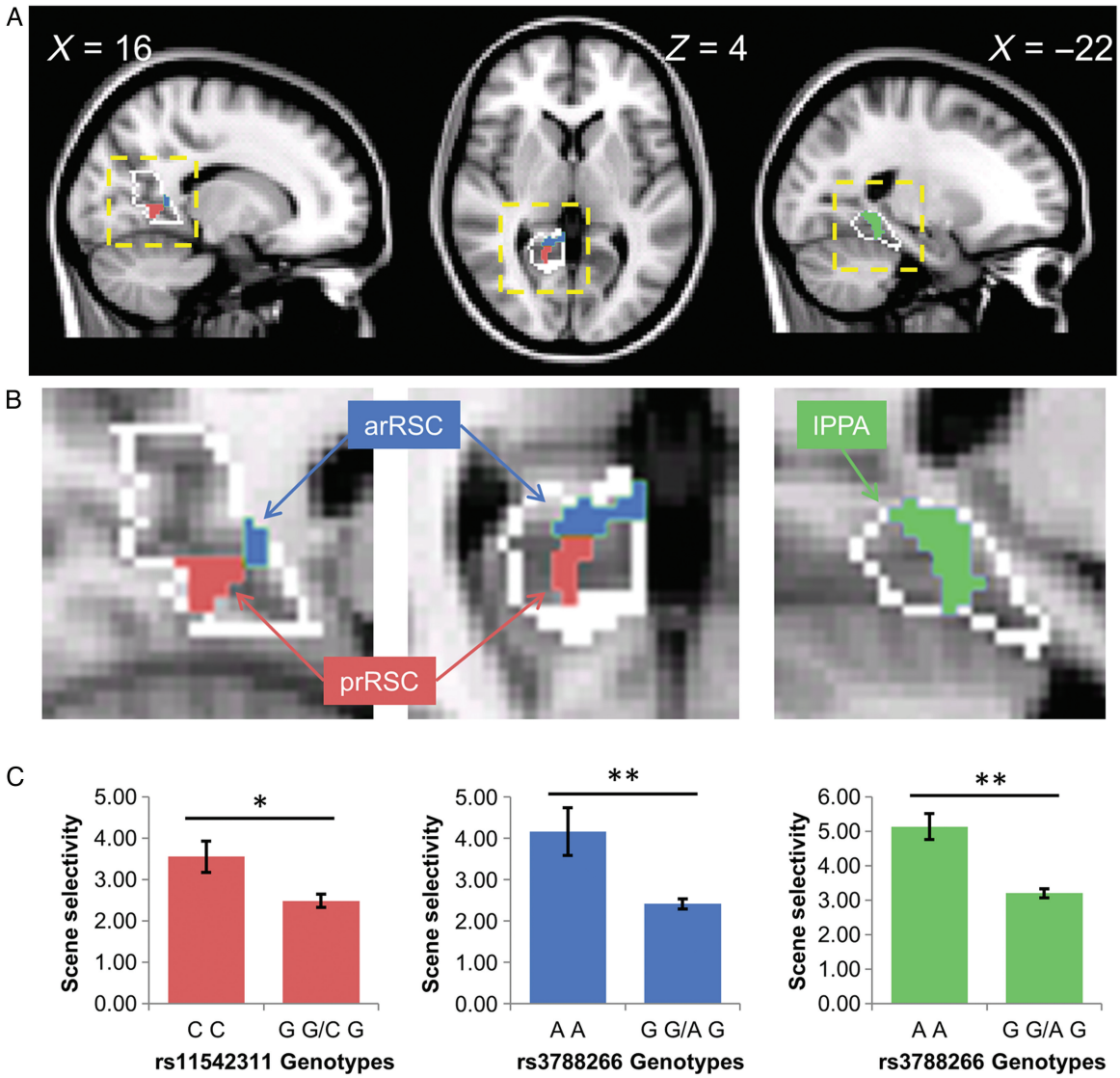

Figure 2. Modulatory Effects of S100B SNPs on scene selectivity in the scene-selective regions. (*A*) Clusters that showed significant associations between scene selectivity and S100B SNPs ($P < 0.05$, cluster corrected), and (*B*) the enlarged views of the regions within the corresponding yellow box above. Red: the posterior part of the right retrosplenial cortex (prRSC) associated with rs11542311; Blue: the anterior part of the right RSC (arRSC) associated with rs3788266; Green: the left parahippocampal place area (lPPA) associated with rs3788266. White line: the region boundaries of the right RSC (left and middle panel) and lPPA (right panel). (*C*) The recessive models for rs11542311 (left panel) and rs3788266 (middle and right panel). *$P < 0.05$; **$P < 0.005$.

and G-allele carries of rs3788266 (beta = 0.57, $P = 0.0008$) was reduced after being adjusted by the mediator of the serum levels of S100B protein (beta = 0.53, $P = 0.019$; Fig. 3C). Further analysis revealed that 8% of the total effect of rs378866 genotype on scene selectivity in the arRSC was mediated by the serum levels of S100B protein. Bootstrapping simulation ($n = 10\,000$) confirmed that the indirect effect though the serum levels of S100B protein was significant ($P < 0.05$) with a 95% CI of 0.004–0.193. That is, the serum levels of S100B protein significantly mediated the association between rs3788266 genotype and the arRSC scene selectivity.

Discussion

In this study, we combined fMRI and multiple modalities of gene data, including gene expression in postmortem brains, gene polymorphisms, and serum levels of gene product (i.e., the S100B protein) and established a reliable link between the S100B gene and cortical processing of navigationally relevant scenes in humans. First, we observed that the spatial pattern of S100B gene expression in postmortem brains was associated with that of the activation map for spatial navigation in general, and for scene processing in particular. Then, in a large cohort of Han Chinese adults, we found that S100B gene polymorphisms (rs3788266 and rs11542311) modulated scene selectivity in the left PPA, anterior, and posterior right RSC, respectively. Finally, we found that the serum levels of S100B protein mediated the association between rs3788266 and the arRSC scene selectivity, suggesting that the S100B gene may modulate cortical scene selectivity through the S100B protein. Together, these convergent findings indicate a functional role for the S100B gene in human spatial navigation.

To the best of our knowledge, this is the first evidence for the effect of the S100B gene on navigation-related cortical activity

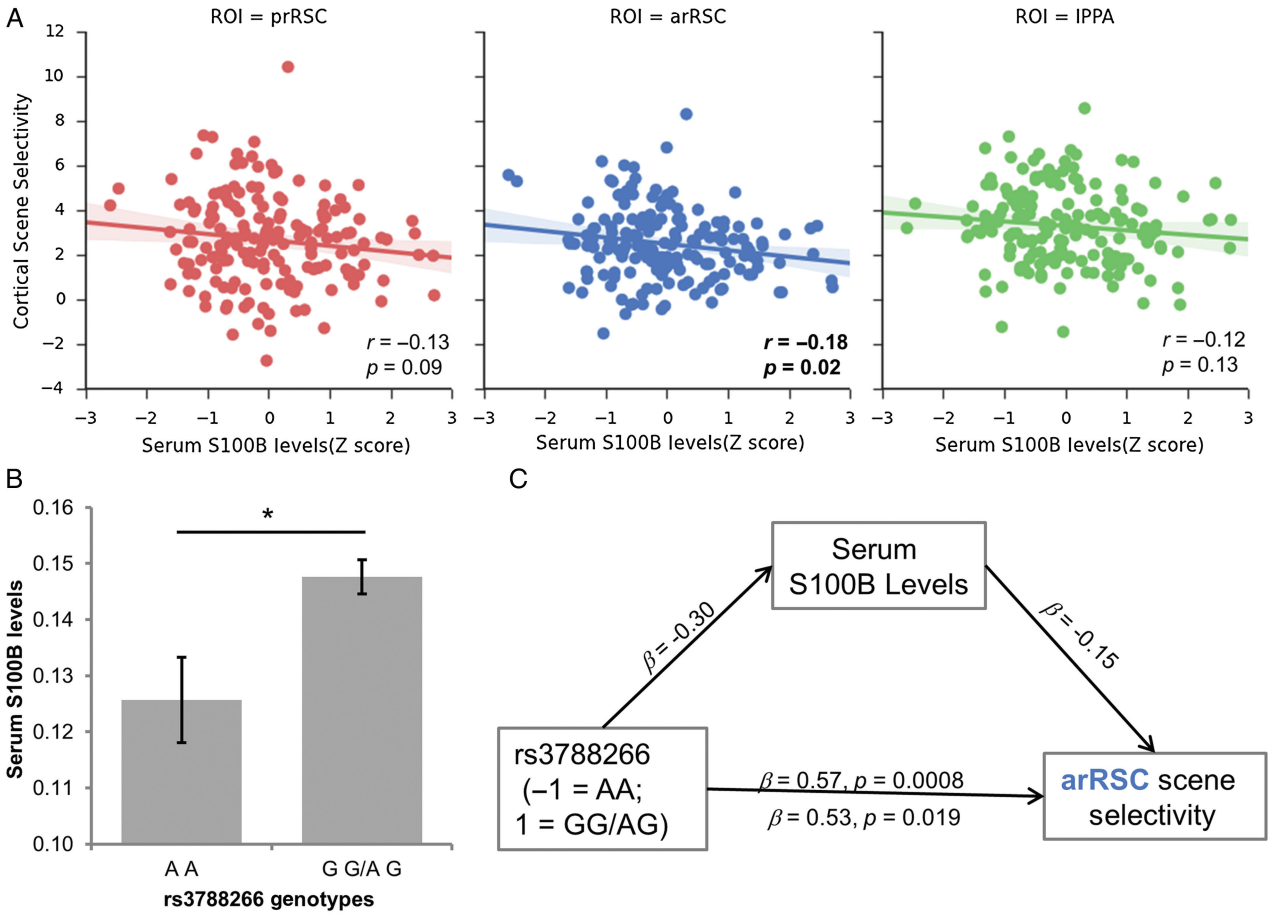

Figure 3. Relationship between S100B SNP, serum levels of S100B protein, and scene selectivity. (A) Correlations between individual's serum S100B levels (with age and sex controlled) and cortical scene selectivity in the prRSC, arRSC, and lPPA. (B) Serum levels of S100B protein in homogenous A-allele carriers and G-allele carries of rs3788266. *$P < 0.05$. (C) Serum levels of S100B protein mediated the association between S100B SNP and scene selectivity in the arRSC.

phenotype in humans. Consistent with our results, previous animal studies have shown that the S100B gene regulates neuronal synaptic activity related to spatial navigation in mice. Specifically, over-expression of human S100B gene in the transgenic mice results in decreased post-tetanic excitatory postsynaptic potentials in hippocampus and impaired spatial learning (Gerlai et al. 1995), whereas mutant mice with null expression of S100B exhibited increased long-term potentiation (LTP) and enhanced spatial ability (Nishiyama et al. 2002). Extending these findings from animals to humans, our study demonstrated the influences of the S100B gene on neural basis supporting spatial navigation in the human brain, and thus, took the first step to illuminate the neurogenetic mechanism of spatial navigation in humans.

In addition, our results echo the spatial ability impairments reported in the psychiatric disorders associated with the S100B gene, and advance previous human studies on the S100B gene in several aspects. First, while previous studies on the S100B gene in humans focused mainly on its involvement in various psychiatric disorders (Schroeter and Steiner 2009), our findings indicate that the S100B gene is implicated not only in pathological brain conditions, but also in normal neural processing of navigation in the healthy population. Moreover, our results indicate that the effect of the S100B gene on neural processing is specific to scene processing, but not to face processing. Given that the scene-selective regions constitute a specialized mechanism for scene recognition in human brain (Epstein and Vass 2014), our finding provides the first evidence that the specialized cortical machinery of scene recognition in human brain is genetically specified and illuminates which specific gene is involved. Note that of the 3 scene-selective regions, we obtained the gene-neural association in the RSC and PPA, but not in the OPA. Although all these regions are involved in scene processing (Epstein et al. 1999; Maguire 2001; Dilks et al. 2013), they appear to play different roles in navigation (Epstein 2008; Park and Chun 2009). A recent study showed that the RSC and OPA are parts of 2 parallel networks that include different connections to the PPA (Nasr et al. 2013). Our results suggest that the S100B gene may modulate scene processing mainly in the RSC-PPA network. Finally, our findings may provide a novel explanation for the spatial impairments in the disorders associated with the S100B gene on a neurogenetic level. Specifically, previous studies have indicated rs3788266 as a risk variant for bipolar affective disorder (BPAD) (Roche et al. 2007), and rs11542311 for schizophrenia (Liu et al. 2005), and serum levels of S100B protein are elevated in BPAD (Machado-Vieira et al. 2002; Andreazza et al. 2007) and schizophrenia (Schroeter and Steiner 2009). Interestingly, impairment in spatial ability has been reported in schizophrenia (Hanlon et al. 2006; Weniger and Irle 2008) and BPAD (Dickstein et al. 2004; Olvera et al. 2005), and S100B gene polymorphisms including rs11542311 can predict performance in spatial tasks in schizophrenia patients (Zhai et al. 2011; Zhai et al. 2012). Our results imply that the spatial deficits in schizophrenia and BPAD may

partly result from the decreased neural activity in response to environmental scenes, especially in the RSC and PPA, associated with the risk alleles of the S100B gene in these patients.

The exact biological mechanism by which the S100B gene may influence cortical scene processing is unknown and remains to be elucidated. Both of the SNPs (rs11542311 and rs3788266) affecting scene selectivity in our study have been shown to exert direct influence on S100B gene expression and serum levels of the S100B protein (Roche et al. 2007; Hohoff et al. 2010; Dagdan et al. 2011), yet we obtained an association only between rs3788266 and serum levels of the S100B protein, possibly due to the modest size of the cohort. This raises the hypothesis that the S100B gene may modulate neural processing of navigation by affecting expression of the S100B protein. As a calcium-binding protein secreted mainly by glia cells, the S100B protein has been thought in previous animal studies to be involved in glia-to-neuron signaling through which glia may play a role in modulating neuronal activity either intracellularly or extracellularly (Donato et al. 2009; Donato et al. 2013). In humans, indeed, we found that the serum levels of S100B protein could predict individual differences in scene selectivity, given that the serum level of S100B protein is an accurate reflection of S100B protein level in human brain tissue (Reiber 2001; Rothermundt et al. 2004). More importantly, our mediation result suggests that rs3788266 may have an impact on scene selectivity in the arRSC through its modulation of S100B protein level. Taken together, we can tentatively speculate that the AA genotype of rs3788266 may produce lower S100B protein level, which lead to higher scene selectivity in the arRSC. Future studies are needed to investigate the cellular and molecular mechanisms by which the S100B protein exerts influences on regional responses in the human brain. On the other hand, scene selectivity in the left PPA and prRSC was modulated by the S100B gene but not associated with the serum levels of S100B protein. This suggests the possibility that, in addition to directly influencing expression of the S100B protein, variations in the S100B gene may also modulate neural processing of navigation by acting in combination with other genetic and environmental factors. This topic warrants further investigation in future studies. Finally, the failure to achieve statistical significance for the association between variation in rs11542311 and serum levels of S100B may be related to the different age distribution or the different sample population used in the current study (Portela et al. 2002; Hohoff et al. 2010). Analysis of larger samples is required to validate the effect of rs11542311 on S100B expression in Han Chinese population.

Notably, correlation coefficients observed in the present study were moderate in general. For example, the correlation coefficients between the S100B gene expression map and the activation maps of spatial navigation and scene processing ranged from 0.2 to 0.3. However, the correlations were stable because 1) the association was consistently observed in all 6 donors and 2) the correlation between the S100B gene expression map and the activation map of face processing failed to reach significance with a similar sample size. Therefore, sample sizes were unlikely the major factor that drove the significance of the correlations. In addition, the level of the correlation between serum S100B levels and scene selectivity reported here (e.g., $r = 0.18$) is in line with a recent study showing a small level of the serum-brain association with a large sample size ($r = 0.18$, $N = 247$) in particular (Jiang et al. 2015), and with other fMRI studies based on a large sample size in general (e.g., Holmes et al. 2012; He et al. 2013; Huang et al. 2014; Kong et al. 2014). The small effect size of the correlations in the present study may reflect the fact that the genetic measures of the S100B used here (i.e., the S100B gene expression in brain and the serum S100B level) are a part of many genetic and environmental factors accounting for the variance in neural basis of scene processing. In addition, the reliability of the measurement of both the fMRI activations and the S100B gene factors (particularly the serum S100B levels) is not perfect, which may further underestimate the strength of the correlations.

Moreover, the differences in scene selectivity for different genotypes of rs3788266 shall be interpreted with caution, because the association was based on Han Chinese, and the AA genotype in rs3788266 is much more common in European population (~25% in population CEU from the HapMap) than in Han Chinese (~5% in the present study). On the other hand, the convergent results across multiple modalities of the datasets with various geographic origins observed here, as well as analogous results in animals (Gerlai et al. 1995; Nishiyama et al. 2002), suggest that the association between S100B gene and scene processing may not be limited to the Han Chinese. The test of the generality of the association awaits future studies with a replication attempt in groups of other geographic origins.

In sum, our results provide convergent evidence for an association between the S100B gene and cortical processing of navigationally relevant scenes, suggesting that S100B gene may play an important role in human navigation. In this study, we adopted a novel discovery-based method which allows researchers to generate hypotheses about the neurogenetic basis of cognitive functions by relating patterns of brain activation with gene expression measured in postmortem brains (see also Gorgolewski et al. [2014]). For the first time, we adopted this method to relate the S100B gene to spatial navigation in humans, which served as a guide for a subsequent investigation in which we established the gene-neural association with a combination of multiple modalities of gene data. Thus, our study suggests the potential applications of the novel method in more imaging genetics studies to provide clues about involvement of candidate genetic factors in other cognitive functions and complex phenotypes. In addition, the current study focused on one component of spatial navigation, scene processing. Future studies are needed to explore whether the S100B gene also modulates other higher-level components of spatial navigation with more complex spatial tasks (Wolbers and Hegarty 2010). Finally, although intermediate phenotypes at the neural level as measured by fMRI are considered more sensitive to genetic influences than phenotypes at the behavioral level (Hariri et al. 2006; Green et al. 2008; Mattay et al. 2008), future studies collecting genetic, neural, and behavioral data in the same group of participants are needed to investigate the complex gene-neural-behavioral interactions in human spatial navigation.

Author contributions

X.Z.K. and J.L. designed the experiments, Y.S. and X.Z.K. conducted the experiments, X.Z.K. and Z.Z. analyzed the data, X.Z.K., Y.S., and J.L. wrote the manuscript, and J.L. supervised the project.

Funding

This study was funded by the National Natural Science Foundation of China (31230031), the National Basic Research Program of China (2014CB846101), the National Natural Science Foundation of China (31221003, 31471067 and 31470055), the National Social Science Foundation of China (13&ZD073, 14ZDB160), and Changjiang Scholars Programme of China.

Notes

Conflict of Interest: None declared.

References

Aguirre GK, D'Esposito M. 1999. Topographical disorientation: a synthesis and taxonomy. Brain. 122(Pt 9):1613–1628.

Aguirre GK, Zarahn E, D'Esposito M. 1998. An area within human ventral cortex sensitive to "building" stimuli: evidence and implications. Neuron. 21:373–383.

Andreazza AC, Cassini C, Rosa AR, Leite MC, de Almeida LM, Nardin P, Cunha AB, Cereser KM, Santin A, Gottfried C, et al. 2007. Serum S100B and antioxidant enzymes in bipolar patients. J Psychiatr Res. 41:523–529.

Dagdan E, Morris DW, Campbell M, Hill M, Rothermundt M, Kastner F, Hohoff C, von Eiff C, Krakowitzky P, Gill M, et al. 2011. Functional assessment of a promoter polymorphism in S100B, a putative risk variant for bipolar disorder. Am J Med Genet B Neuropsychiatr Genet. 156B:691–699.

de Bakker PI, Yelensky R, Pe'er I, Gabriel SB, Daly MJ, Altshuler D. 2005. Efficiency and power in genetic association studies. Nat Genet. 37:1217–1223.

Dickstein DP, Treland JE, Snow J, McClure EB, Mehta MS, Towbin KE, Pine DS, Leibenluft E. 2004. Neuropsychological performance in pediatric bipolar disorder. Biol Psychiatry. 55:32–39.

Dilks DD, Julian JB, Paunov AM, Kanwisher N. 2013. The occipital place area is causally and selectively involved in scene perception. J Neurosci. 33:1331–1336a.

Donato R, Cannon BR, Sorci G, Riuzzi F, Hsu K, Weber DJ, Geczy CL. 2013. Functions of S100 proteins. Curr Mol Med. 13:24–57.

Donato R, Sorci G, Riuzzi F, Arcuri C, Bianchi R, Brozzi F, Tubaro C, Giambanco I. 2009. S100B's double life: intracellular regulator and extracellular signal. Biochim Biophys Acta. 1793:1008–1022.

Epstein R, Deyoe EA, Press DZ, Rosen AC, Kanwisher N. 2001. Neuropsychological evidence for a topographical learning mechanism in parahippocampal cortex. Cogn Neuropsychol. 18:481–508.

Epstein R, Harris A, Stanley D, Kanwisher N. 1999. The parahippocampal place area: recognition, navigation, or encoding? Neuron. 23:115–125.

Epstein R, Kanwisher N. 1998. A cortical representation of the local visual environment. Nature. 392:598–601.

Epstein RA. 2008. Parahippocampal and retrosplenial contributions to human spatial navigation. Trends Cogn Sci. 12:388–396.

Epstein RA, Vass LK. 2014. Neural systems for landmark-based wayfinding in humans. Philos Trans R Soc Lond B Biol Sci. 369:20120533.

Gerlai R, Wojtowicz JM, Marks A, Roder J. 1995. Overexpression of a calcium-binding protein, S100 beta, in astrocytes alters synaptic plasticity and impairs spatial learning in transgenic mice. Learn Mem. 2:26–39.

Ghaem O, Mellet E, Crivello F, Tzourio N, Mazoyer B, Berthoz A, Denis M. 1997. Mental navigation along memorized routes activates the hippocampus, precuneus, and insula. Neuroreport. 8:739–744.

Gorgolewski K, Fox A, Chang L, Schäfer A, Arélin K, Burmann I, Sacher J, Margulies D. 2014. Tight fitting genes: Finding relations between statistical maps and gene expression patterns. In. Organization for Human Brain Mapping. Hamburg, Germany.

Green AE, Munafo MR, DeYoung CG, Fossella JA, Fan J, Gray JR. 2008. Using genetic data in cognitive neuroscience: from growing pains to genuine insights. Nat Rev Neurosci. 9:710–720.

Grill-Spector K. 2003. The neural basis of object perception. Curr Opin Neurobiol. 13:159–166.

Hanlon FM, Weisend MP, Hamilton DA, Jones AP, Thoma RJ, Huang M, Martin K, Yeo RA, Miller GA, Canive JM. 2006. Impairment on the hippocampal-dependent virtual Morris water task in schizophrenia. Schizophr Res. 87:67–80.

Hariri AR, Drabant EM, Weinberger DR. 2006. Imaging genetics: perspectives from studies of genetically driven variation in serotonin function and corticolimbic affective processing. Biol Psychiatry. 59:888–897.

Hasson U, Harel M, Levy I, Malach R. 2003. Large-scale mirror-symmetry organization of human occipito-temporal object areas. Neuron. 37:1027–1041.

Hawrylycz MJ, Lein ES, Guillozet-Bongaarts AL, Shen EH, Ng L, Miller JA, van de Lagemaat LN, Smith KA, Ebbert A, Riley ZL, et al. 2012. An anatomically comprehensive atlas of the adult human brain transcriptome. Nature. 489:391–399.

He Q, Xue G, Chen C, Lu ZL, Dong Q. 2013. Decoding the neuroanatomical basis of reading ability: a multivoxel morphometric study. J Neurosci. 33:12835–12843.

Helfinstein SM, Schonberg T, Congdon E, Karlsgodt KH, Mumford JA, Sabb FW, Cannon TD, London ED, Bilder RM, Poldrack RA. 2014. Predicting risky choices from brain activity patterns. Proc Natl Acad Sci USA. 111:2470–2475.

Hohoff C, Ponath G, Freitag CM, Kastner F, Krakowitzky P, Domschke K, Koelkebeck K, Kipp F, von Eiff C, Deckert J, et al. 2010. Risk variants in the S100B gene predict elevated S100B serum concentrations in healthy individuals. Am J Med Genet B Neuropsychiatr Genet. 153B:291–297.

Holmes AJ, Lee PH, Hollinshead MO, Bakst L, Roffman JL, Smoller JW, Buckner RL. 2012. Individual differences in amygdala-medial prefrontal anatomy link negative affect, impaired social functioning, and polygenic depression risk. J Neurosci. 32:18087–18100.

Huang L, Song Y, Li J, Zhen Z, Yang Z, Liu J. 2014. Individual differences in cortical face selectivity predict behavioral performance in face recognition. Front Hum Neurosci. 8:483.

Ino T, Inoue Y, Kage M, Hirose S, Kimura T, Fukuyama H. 2002. Mental navigation in humans is processed in the anterior bank of the parieto-occipital sulcus. Neurosci Lett. 322:182–186.

Jiang JY, Wen W, Brown DA, Crawford J, Thalamuthu A, Smith E, Breit SN, Liu T, Zhu WL, Brodaty H, et al. 2015. The Relationship of Serum Macrophage Inhibitory Cytokine-1 Levels with Gray Matter Volumes in Community-Dwelling Older Individuals. PLoS One. 10:e0123399.

Kong XZ, Zhen Z, Li X, Lu HH, Wang R, Liu L, He Y, Zang Y, Liu J. 2014. Individual differences in impulsivity predict head motion during magnetic resonance imaging. PLoS One. 9: e104989.

Liu J, Shi Y, Tang J, Guo T, Li X, Yang Y, Chen Q, Zhao X, He G, Feng G, et al. 2005. SNPs and haplotypes in the S100B gene reveal association with schizophrenia. Biochem Biophys Res Commun. 328:335–341.

Machado-Vieira R, Lara DR, Portela LV, Goncalves CA, Soares JC, Kapczinski F, Souza DO. 2002. Elevated serum S100B protein in drug-free bipolar patients during first manic episode: a pilot study. Eur Neuropsychopharmacol. 12:269–272.

MacKinnon DP, Fairchild AJ, Fritz MS. 2007. Mediation analysis. Annu Rev Psychol. 58:593–614.

Maguire EA. 2001. The retrosplenial contribution to human navigation: a review of lesion and neuroimaging findings. Scand J Psychol. 42:225–238.

Maguire EA, Burgess N, Donnett JG, Frackowiak RS, Frith CD, O'Keefe J. 1998. Knowing where and getting there: a human navigation network. Science. 280:921–924.

Mattay VS, Goldberg TE, Sambataro F, Weinberger DR. 2008. Neurobiology of cognitive aging: insights from imaging genetics. Biol Psychol. 79:9–22.

Mendez MF, Cherrier MM. 2003. Agnosia for scenes in topographagnosia. Neuropsychologia. 41:1387–1395.
Nakamura K, Kawashima R, Sato N, Nakamura A, Sugiura M, Kato T, Hatano K, Ito K, Fukuda H, Schormann T, et al. 2000. Functional delineation of the human occipito-temporal areas related to face and scene processing. A PET Study Brain. 123(Pt 9):1903–1912.
Nasr S, Devaney KJ, Tootell RB. 2013. Spatial encoding and underlying circuitry in scene-selective cortex. Neuroimage. 83:892–900.
Nishiyama H, Knopfel T, Endo S, Itohara S. 2002. Glial protein S100B modulates long-term neuronal synaptic plasticity. Proc Natl Acad Sci USA. 99:4037–4042.
Ohnishi T, Matsuda H, Hirakata M, Ugawa Y. 2006. Navigation ability dependent neural activation in the human brain: an fMRI study. Neurosci Res. 55:361–369.
Olvera RL, Semrud-Clikeman M, Pliszka SR, O'Donnell L. 2005. Neuropsychological deficits in adolescents with conduct disorder and comorbid bipolar disorder: a pilot study. Bipolar Disord. 7:57–67.
Park S, Chun MM. 2009. Different roles of the parahippocampal place area (PPA) and retrosplenial cortex (RSC) in panoramic scene perception. Neuroimage. 47:1747–1756.
Pitcher D, Dilks DD, Saxe RR, Triantafyllou C, Kanwisher N. 2011. Differential selectivity for dynamic versus static information in face-selective cortical regions. Neuroimage. 56:2356–2363.
Portela LV, Tort AB, Schaf DV, Ribeiro L, Nora DB, Walz R, Rotta LN, Silva CT, Busnello JV, Kapczinski F, et al. 2002. The serum S100B concentration is age dependent. Clin Chem. 48:950–952.
Purcell S, Neale B, Todd-Brown K, Thomas L, Ferreira MA, Bender D, Maller J, Sklar P, de Bakker PI, Daly MJ, et al. 2007. PLINK: a tool set for whole-genome association and population-based linkage analyses. Am J Hum Genet. 81:559–575.
Qi LY, Xiu MH, Chen da C, Wang F, Kosten TA, Kosten TR, Zhang XY. 2009. Increased serum S100B levels in chronic schizophrenic patients on long-term clozapine or typical antipsychotics. Neurosci Lett. 462:113–117.
Rauchs G, Orban P, Balteau E, Schmidt C, Degueldre C, Luxen A, Maquet P, Peigneux P. 2008. Partially segregated neural networks for spatial and contextual memory in virtual navigation. Hippocampus. 18:503–518.
Reiber H. 2001. Dynamics of brain-derived proteins in cerebrospinal fluid. Clin Chim Acta. 310:173–186.
Roche S, Cassidy F, Zhao C, Badger J, Claffey E, Mooney L, Delaney C, Dobrin S, McKeon P. 2007. Candidate gene analysis of 21q22: support for S100B as a susceptibility gene for bipolar affective disorder with psychosis. Am J Med Genet B Neuropsychiatr Genet. 144B:1094–1096.
Rosenbaum RS, Ziegler M, Winocur G, Grady CL, Moscovitch M. 2004. "I have often walked down this street before": fMRI studies on the hippocampus and other structures during mental navigation of an old environment. Hippocampus. 14:826–835.
Rothermundt M, Falkai P, Ponath G, Abel S, Burkle H, Diedrich M, Hetzel G, Peters M, Siegmund A, Pedersen A, et al. 2004. Glial cell dysfunction in schizophrenia indicated by increased S100B in the CSF. Mol Psychiatry. 9:897–899.
Schroeter ML, Steiner J. 2009. Elevated serum levels of the glial marker protein S100B are not specific for schizophrenia or mood disorders. Mol Psychiatry. 14:235–237.
Shah P, Miyake A editors. 2005. The Cambridge handbook of visuospatial thinking. Cambridge: University Press.
Sherrill KR, Erdem UM, Ross RS, Brown TI, Hasselmo ME, Stern CE. 2013. Hippocampus and retrosplenial cortex combine path integration signals for successful navigation. J Neurosci. 33:19304–19313.
Spiers HJ, Maguire EA. 2006. Thoughts, behaviour, and brain dynamics during navigation in the real world. Neuroimage. 31:1826–1840.
Wager TD, Davidson ML, Hughes BL, Lindquist MA, Ochsner KN. 2008. Prefrontal-subcortical pathways mediating successful emotion regulation. Neuron. 59:1037–1050.
Ward BD. Simultaneous inference for FMRI data. 2000. Available from: http://afni.nimh.nih.gov/pub/dist/doc/manual/AlphaSim.pdf.
Weniger G, Irle E. 2008. Allocentric memory impaired and egocentric memory intact as assessed by virtual reality in recent-onset schizophrenia. Schizophr Res. 101:201–209.
Wolbers T, Hegarty M. 2010. What determines our navigational abilities? Trends Cogn Sci. 14:138–146.
Yarkoni T, Poldrack RA, Nichols TE, Van Essen DC, Wager TD. 2011. Large-scale automated synthesis of human functional neuroimaging data. Nat Methods. 8:665–670.
Zhai J, Cheng L, Dong J, Shen Q, Zhang Q, Chen M, Gao L, Chen X, Wang K, Deng X, et al. 2012. S100B gene polymorphisms predict prefrontal spatial function in both schizophrenia patients and healthy individuals. Schizophr Res. 134:89–94.
Zhai J, Zhang Q, Cheng L, Chen M, Wang K, Liu Y, Deng X, Chen X, Shen Q, Xu Z, et al. 2011. Risk variants in the S100B gene, associated with elevated S100B levels, are also associated with visuospatial disability of schizophrenia. Behav Brain Res. 217:363–368.
Zhen Z, Fang H, Liu J. 2013. The hierarchical brain network for face recognition. PLoS One. 8:e59886.
Zhen Z, Yang Z, Huang L, Kong XZ, Wang X, Dang X, Huang Y, Song Y, Liu J. 2015. Quantifying interindividual variability and asymmetry of face-selective regions: a probabilistic functional atlas. Neuroimage. 113:13–25.